Downloaded via UNIV OF COLORADO BOULDER on March 14, 2019 at 16:51:04 (UTC). See https://pubs.acs.org/sharingguidelines for options on how to legitimately share published articles.

Design of a De Novo Aggregating Antimicrobial Peptide and a **Bacterial Conjugation-Based Delivery System**

Logan T. Collins, Peter B. Otoupal, Jocelyn K. Campos, Colleen M. Courtney, and Anushree Chatterjee*

Department of Chemical and Biological Engineering, University of Colorado, Boulder, Colorado 80303, United States

Supporting Information

ABSTRACT: Antibacterial resistance necessitates the development of novel treatment methods for infections. Protein aggregates have recently been applied as antimicrobials to disrupt bacterial homeostasis. Past work on protein aggregates has focused on genome mining for aggregation-prone sequences in bacterial genomes rather than on rational design of aggregating antimicrobial peptides. Here, we use a synthetic biology approach to design an artificial gene encoding a de novo aggregating antimicrobial peptide. This artificial gene, opaL (overexpressed protein aggregator lipophilic), disrupts bacterial homeostasis by expressing extremely hydrophobic peptides. When this hydrophobic sequence is disrupted by acidic residues, consequent aggregation and antimicrobial effect decrease. Further, we developed a probiotic delivery system using the broad-host range conjugative plasmid RK2 to transfer the gene from donor to recipient bacteria. We utilize RK2 to mobilize a shuttle plasmid carrying opaL by adding the RK2 origin of transfer. We show that opaL is nontoxic to the donor, allowing for maintenance and transfer since its expression is under control of a promoter with a recipient-specific T7 RNA polymerase. Upon mating of donor and recipient Escherichia coli, we observe selective growth repression in T7 polymerase-expressing recipients. This technique could be used to target desired pathogens by selecting pathogen-specific promoters to control T7 RNA polymerase expression and provides a basis for the design and delivery of aggregating antimicrobial peptides.

ntibacterial resistance represents a growing public health Athreat. Resistant bacteria can cause infections that are untreatable with most or all current antibiotics. For instance, carbapenem-resistant enterobacteriaceae have been reported in nations including the United States, India, United Kingdom, and others. Here, we develop a novel de novo aggregating antimicrobial peptide (AMP) and repurpose an RK2-mediated bacterial conjugation system to deliver the gene encoding this peptide.

The toxicity of aggregating peptides arises from disruptive interaction of exposed hydrophobic side chains with cellular proteins, induction of oxidative stress, overload of proteolytic machinery, and coaggregation with endogenous macromolecules.² Instead of binding a particular macromolecular target site, aggregating AMPs cause widespread disruption of homeostasis in bacteria, potentially slowing resistance since many resistant phenotypes involve target site alterations. Bednarska et al. and Khodaparast et al. demonstrated the promise of aggregating AMPs 3,4 using peptides derived from existing bacterial protein sequences by predicting aggregation propensity with the statistical thermodynamics algorithm TANGO.⁵ A small fraction of the screened peptides showed significant antibacterial activity. However, the approaches were limited since the peptides were derived from naturally occurring bacterial sequences and required screening of numerous candidates. Even the successful peptides were shown to lose function upon sequence rearrangements, indicating that they would not be amenable to directed evolution efforts which otherwise could restore activity if resistance was to arise.

We rationally design a de novo aggregating antimicrobial peptide, OpaL (overexpressed protein aggregator lipophilic), by choosing numerous hydrophobic amino acid residues to maximize protein aggregation (Figure 1A). To the best of our knowledge, OpaL represents the first aggregating antimicrobial peptide designed without using pre-existing sequences found in nature. We show that OpaL causes aggregation in bacteria and exhibits a bactericidal effect. We use the conjugative plasmid RK2 to transfer a pET11a-opaL shuttle plasmid from donor to recipient bacteria and target the strain of interest via a strainspecific promoter. Our work provides a new therapeutic strategy with potential clinical applications.

OpaL's sequence was manually constructed while considering design parameters around hydrophobic aggregation and intracellular half-life (Figure 1A). To promote insolubility, 139 amino acids of OpaL's 185 residue sequence (75.1%) possess hydrophobic side chains. These include 4 (2.2%) alanine, 15 (8.1%) cysteine, 53 (28.6%) isoleucine, 17 (9.2%) methionine, 14 (7.6%) proline, and 36 (19.5%) valine (Figure 1B). As long stretches of hydrophobic residues further promote aggregation,6 most of OpaL consists of consecutive nonpolar amino acid sequences, though intermittent glycines were included since increased conformational flexibility has also been known to increase aggregate formation when hydrophobic amino acids are prevalent.^{7,8} OpaL was made to be relatively large (with a molecular weight of about 18.5 kDa) compared to

Special Issue: The Chemistry of Synthetic Biology

Received: August 23, 2018 Revised: November 4, 2018 Published: November 7, 2018

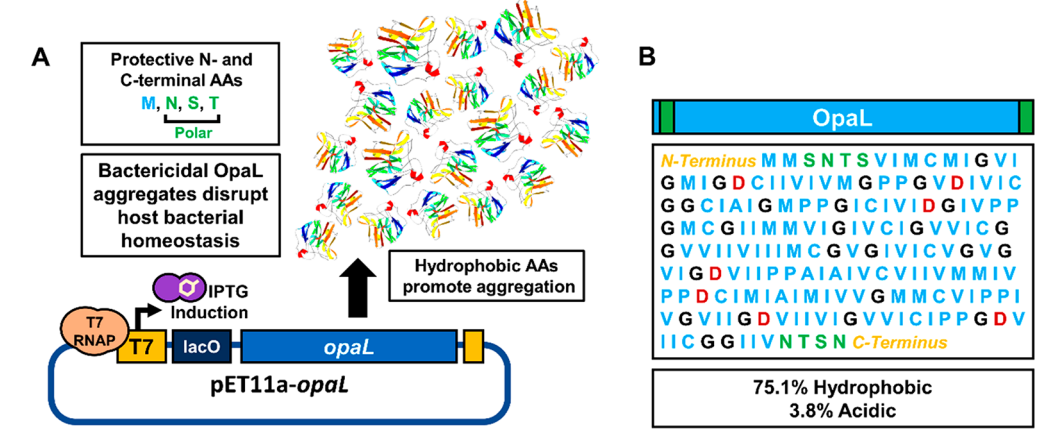


Figure 1. Rational design of OpaL. (A) The pET11a-opaL vector expresses OpaL from the T7 promoter and so restricts expression to the target strain, BL21 (DE3). Polar terminal patches were incorporated in OpaL to increase OpaL's intracellular half-life. ¹⁰ Numerous (75.1%) hydrophobic residues facilitate formation of toxic intracellular aggregates. ^{2,13} (B) OpaL's primary amino acid sequence with hydrophobic amino acids in blue, glycines in black, aspartic acids in red, and polar amino acids in green.

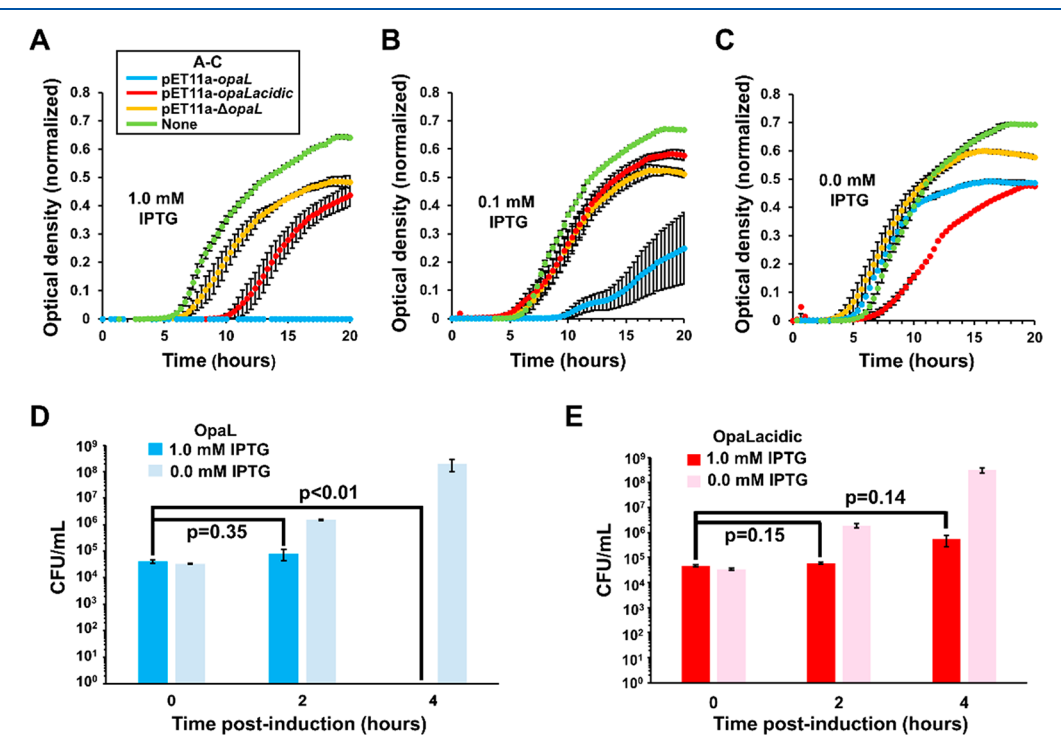


Figure 2. Antimicrobial effect of OpaL. (A–C) Growth curves of BL21 (DE3) carrying plasmids as labeled under (A) 1.0 mM IPTG induction, (B) 0.1 mM IPTG induction, and (C) without IPTG induction. (D) CFUs of BL21 (DE3) carrying pET11a-opaL at t = 0, t = 2, and t = 4 h post induction with 1.0 mM IPTG and at the same time points without IPTG. (E) CFUs of BL21 (DE3) carrying pET11a-opaL acidic at t = 0, t = 2, and t = 4 h post induction with 1.0 mM IPTG and without IPTG. These data represent the means of three biological replicates. Error bars represent standard error, and P values were calculated using a two-tailed type II t test.

many antimicrobial peptides because amorphous aggregates are favored for larger proteins. Terminal polar amino acids (serine, asparagine, and threonine) were incorporated to avoid degradation by proteases that vastly shorten protein half-lives by recognizing bulky terminal hydrophobic residues. N-Formylmethionine was still allowed at the N-terminus since, despite its hydrophobicity, N-formylmethionine promotes long protein half-lives. Since the N-formylmethionine found in bacterial proteins is often cleaved by proteases, the next several chosen residues were also among those which promote long half-lives. OpaL's hydrophobicity-centered design leaves it amenable to a rich array of sequence variations since a large

number of possible rearrangements would still retain OpaL's extremely hydrophobic character and therefore opens the door to the development of a new class of aggregating antimicrobial peptide.

We also created a similar 184 residue control peptide called OpaLacidic, which possesses markedly less potential for hydrophobic aggregation. OpaLacidic includes 30 aspartic acid residues comprising 16.3% of the sequence (Figure S1). To facilitate charge—charge repulsion and interfere with hydrophobic aggregation, these aspartic acids were placed every five residues over most of the sequence. This peptide

served to highlight the importance of OpaL's hydrophobic aggregation mechanism.

We demonstrated OpaL's intracellular toxicity by expressing it from the strong T7 promoter on the pET11a-opaL shuttle plasmid in E. coli BL21 (DE3). In pET11a-derived vectors, a lac operator is located downstream of the T7 promoter, allowing induction with isopropyl β -D-1-thiogalactopyranoside (IPTG) (Figure 1A). When measuring the optical density (OD) of bacterial cultures of BL21 (DE3) carrying pET11aopaL, OpaL expression with 1.0 mM IPTG completely precluded growth (Figure 2A). With 0.1 mM IPTG, OpaL expression decreased mean OD (Figure 2B), but some growth occurred. Without IPTG, BL21 (DE3) carrying pET11a-opaL showed a longer lag time compared to BL21 (DE3) not carrying any plasmids, potentially due to leaky expression from the opaL gene (Figure 2C). BL21 (DE3) expressing OpaLacidic displayed a significantly lower toxicity than OpaL, albeit with lengthened lag times relative to control bacteria not carrying any plasmids (Figure 2A-C). To further investigate this, we deleted the open reading frame of opaL to create the control plasmid pET11a-ΔopaL. BL21 (DE3) carrying pET11a-ΔopaL demonstrated significantly higher growth than cells expressing OpaL or OpaLacidic, although upon induction (0.1 and 1.0 mM IPTG) a lower growth plateau and longer lag time were observed compared to the control without any plasmid (Figure 2A,B) possibly due to metabolic burden from the transcription of short RNAs containing any remaining sequence between the promoter and terminator that was not deleted.

In colony-forming unit (CFU) experiments, viable cell counts of BL21 (DE3) expressing OpaL dropped to zero after 4 h of induction with 1.0 mM IPTG (p < 0.01), indicating a bactericidal mechanism of action (Figure 2D). Without IPTG, the viable cell count continued to increase significantly over time. Viable cell counts after 2 and 4 h for BL21 (DE3) carrying pET11a-opaLacidic remained relatively constant (p > 0.05) with 1.0 mM IPTG, indicating a weaker bacteriostatic effect compared to OpaL (Figure 2E). Without IPTG, bacterial CFU increased over time. These results confirm the antibacterial effect of OpaL.

To computationally test OpaL's aggregation, we employed the statistical thermodynamics algorithm TANGO.⁵ OpaL showed an extremely high mean aggregation propensity of 35.7% (values greater than 5% predict aggregation). OpaLacidic showed a low mean aggregation propensity of 0.7% (Figure 3A, Table S2). These data support OpaL's formation of hydrophobic aggregates. We also used QUARK, an ab initio protein structure prediction tool, to predict the tertiary structures of OpaL and OpaLacidic. DeepView was employed to visualize these structures and compute their solvent-exposed hydrophobic surface areas. OpaL was predicted to be rich in β -sheet structures (Figure 3B), while OpaLacidic was mostly composed of unstructured loops (Figure 3C). OpaL's greater antibacterial toxicity relative to OpaLacidic is consistent with these results since many pathological protein aggregates are also rich in β -sheets. 5,12 OpaL's predicted structure demonstrated 43.6% hydrophobic surface area, while OpaLacidic demonstrated a predicted hydrophobic surface area of 21.2% (Figure 3B,C).

Again, OpaL's higher antibacterial toxicity relative to OpaLacidic is consistent with these results since protein aggregation is known to be heavily dependent on hydrophobicity. ^{2,5,13}

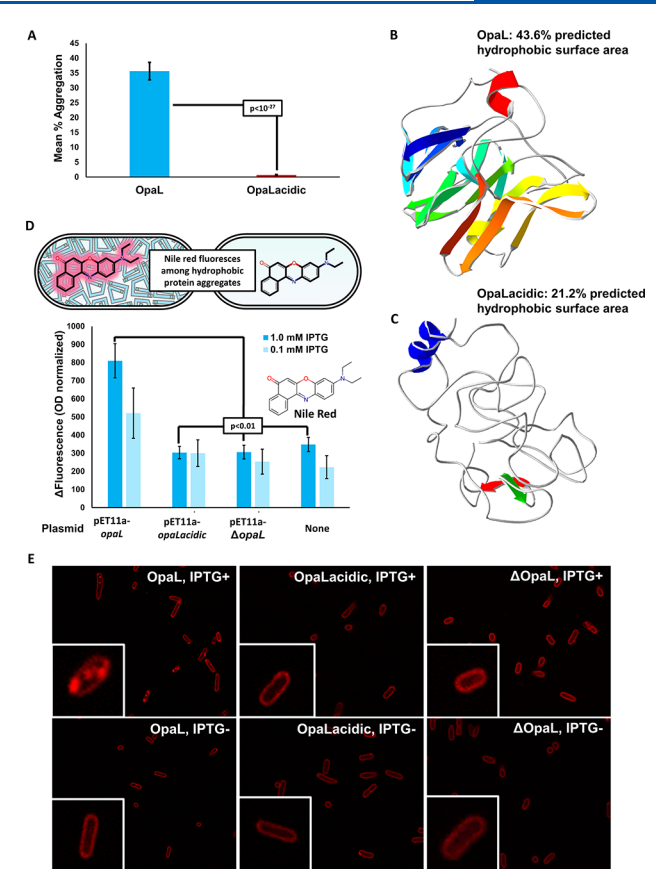


Figure 3. OpaL causes intracellular aggregate formation. (A) Predicted mean aggregation propensity percentages for OpaL and OpaLacidic using the TANGO algorithm. (B) OpaL's structure as predicted by the QUARK algorithm. (C) The structure of OpaLacidic as predicted by QUARK. (D) BL21 (DE3) carrying plasmids as labeled were stained with Nile Red to show that OpaL forms hydrophobic aggregates. These data represent the means of five biological replicates. Error bars represent standard error, and *P* values were calculated using a two-tailed type II *t* test. (E) Intracellular OpaL aggregates visualized with fluorescence microscopy and Nile Red. Aggregates are visible in the bacteria expressing OpaL (top left panel), but not in the controls.

To provide experimental evidence for OpaL's aggregation, we performed an aggregation assay by staining host BL21 (DE3) with the dye Nile Red, which fluoresces upon exposure to hydrophobic environments. 14 After induction with 1.0 mM IPTG, cells carrying pET11a-opaL showed significantly greater increases in fluorescence relative to cells with pET11aopaLacidic, pET11a-ΔopaL, or cells without any plasmids (p < 0.01) (Figure 3D). After induction with 0.1 mM IPTG, cells expressing OpaL showed higher increases in fluorescence relative to the other groups, though the differences were not statistically significant. These results are consistent with the data from TANGO and QUARK, further supporting OpaL's mechanism of hydrophobic aggregation. We also extracted total and soluble protein fractions from strains expressing OpaL, OpaLacidic, and Δ OpaL (Figure S3A,B). The insoluble protein fraction showed substantially more bands (and higher intensity bands) only with expression of OpaL (Figure S3A), while the soluble fraction remained similar for OpaL, OpaLacidic, and Δ OpaL strains (Figure S3B). Finally, we used laser scanning confocal fluorescence microscopy to directly visualize intracellular OpaL aggregates stained with

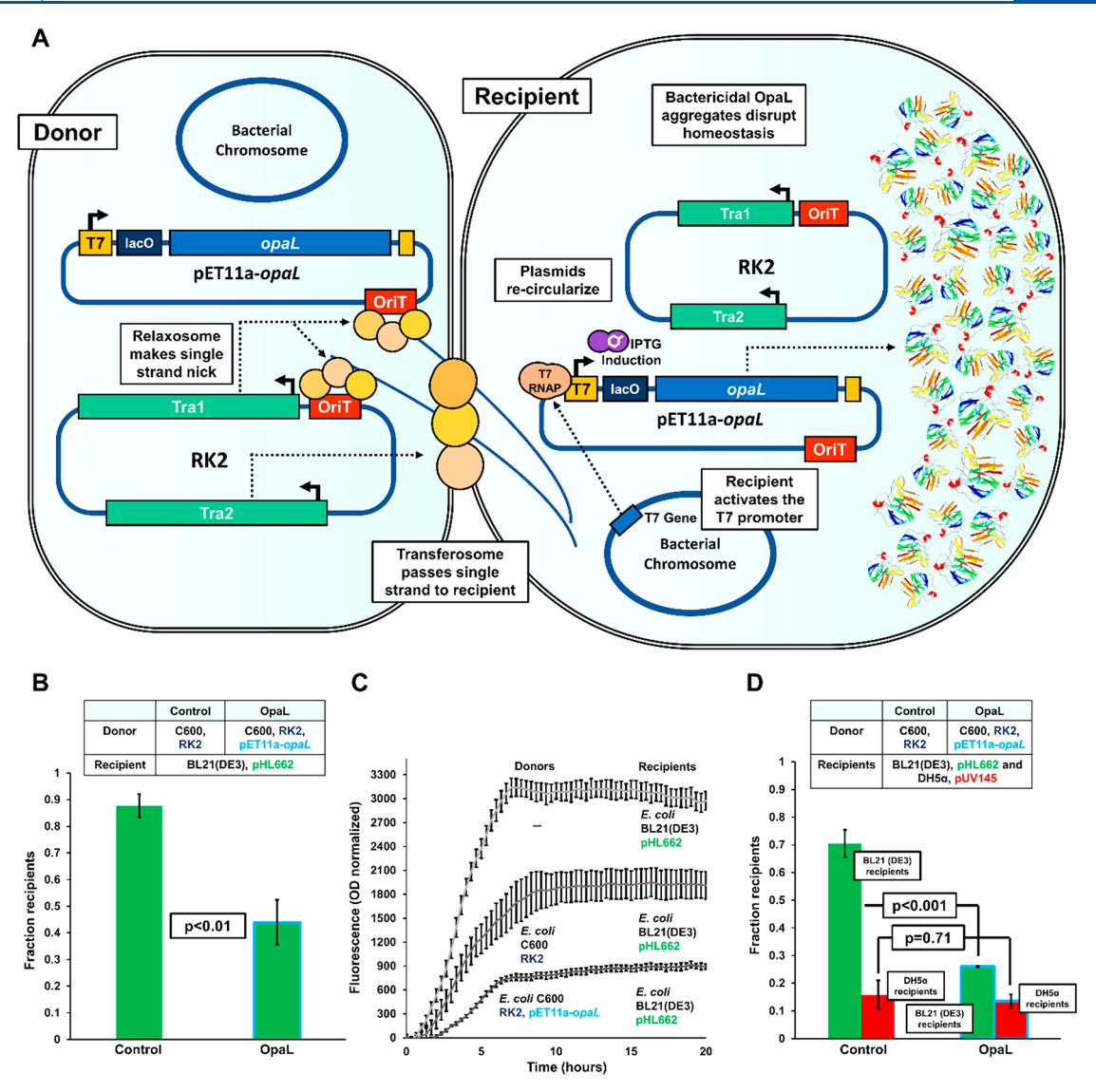


Figure 4. OpaL shows targeted killing when delivered by bacterial conjugation. (A) Donor bacteria transfer the broad-host range conjugative plasmid RK2 and the shuttle plasmid pET11a-opaL to recipient bacteria. RK2 encodes a relaxosome complex, which makes a single-stranded nick in the origin of transfer (OriT),²⁰ and a transferosome complex, which facilitates the transfer of the ssDNA to the recipient. The 450 bp OriT sequence from RK2 was cloned into pET11a-opaL to facilitate conjugative transfer of opaL. BL21 (DE3) encodes T7 RNA polymerase, which binds the T7 promoter upstream of opaL and initiates expression, allowing OpaL to kill the targeted host bacterium. (B) Two-strain CFU mating-toxicity assay as measured by the ratio of BL21 (DE3) recipient CFU/mL to total CFU/mL. (C) Two-strain growth curve mating-toxicity assay measured via recipient GFP fluorescence normalized to OD. These data represent the means of four biological replicates, and error bars represent standard error. (D) Three-strain CFU mating-toxicity assay as measured by the ratios of BL21 (DE3) recipient CFU/mL to total CFU/mL and DH5α nontarget recipient CFU/mL to total CFU/mL. For panels B and D, the mean recipient fractions relative to total cells are displayed. The data represent the means of three biological replicates, error bars represent standard error, and P-values were calculated using a two-tailed type II t test.

Nile Red (Figure 3E). Bacteria expressing OpaL exhibited visible inclusion body formation, while aggregates were not observed in controls with OpaLacidic and Δ OpaL.

We show that bacterial conjugation facilitates delivery of *opaL*-carrying donor cells to targeted BL21 (DE3) recipient cells that express the T7 RNA polymerase (Figure 4A). To mobilize *opaL*, we chose the RK2 plasmid for its high transfer frequency, conjugative promiscuity, and stability. To deliver *opaL* into recipient cells, we designed the pET11a-*opaL* shuttle plasmid, which includes a 450 bp sequence identical to the origin of transfer (OriT) site in RK2¹⁷ and a chloramphenicol (*Cm*) resistance gene (Figure S2). We cotransformed both RK2 and pET11a-*opaL* into *E. coli* C600

to create donor cells. Since *E. coli* C600 do not express T7 polymerase, OpaL expression does not occur in host donor cells. Future extensions of this may allow promoter-based targeting of pathogenic microorganisms via pathogen-specific expression of T7 RNA polymerase. We confirmed that, when mobilized by RK2, pET11a-opaL is transferred conjugatively by measuring mating frequency between donor and recipient cells $(2.63 \times 10^{-2} \pm 1.23 \times 10^{-2} \text{ transconjugants per recipient})$.

We mated donor *E. coli* C600 carrying RK2 and pET11a-opaL plasmids with recipient BL21 (DE3) carrying the GFP-expressing pHL662 plasmid using OD-adjusted 1:3 donor to recipient ratios and 1.0 mM IPTG. GFP fluorescence was

employed to distinguish between strains (Figure S4A). Ratios of recipient colonies to total colonies were computed. The experimental group's recipient CFU fractions were 2.0-fold lower than the fractions of the mating control in which donors only carried RK2 (p < 0.01) (Figure 4B). We also measured recipient growth curves using GFP fluorescence from mating cultures in a microplate reader. Recipient BL21 (DE3) demonstrated a significantly lower growth when donors delivered both RK2 and pET11a-opaL compared to the control (Figure 4C) (p < 0.001).

We performed three-strain matings between donor C600 carrying RK2 and pET11a-opaL plasmids, targeted recipient BL21 (DE3) with pHL662, and nontarget recipient E. coli DH5 α expressing mCherry from the pUV145 plasmid¹⁸ (Figure S4B) using a 1:1:2 OD-adjusted ratio of targeted recipients to nontarget recipients to donors. The ratio was chosen because it gives an approximately equal number of donor cells relative to total recipient cells. Fractions of targeted recipients and fractions of nontarget recipients were determined relative to total colonies on each plate. The experimental group's targeted recipient CFU fractions were 2.7-fold lower than those in the mating control (p < 0.001), while the nontarget recipient CFU fractions were not significantly different from the control (p = 0.71) (Figure 4D).

We designed and tested OpaL as a basis for rational design of novel antimicrobials. Aggregating peptides offer a new approach to addressing bacterial resistance, since unlike smallmolecule antibiotics, hydrophobic aggregates disrupt homeostasis rather than binding to a specific macromolecular target site.^{2,13} Furthermore, insoluble aggregates may show less susceptibility to efflux and OpaL's de novo character may decrease the frequency of enzymatic exaptation toward specific binding and cleavage of sequence motifs. Even if resistance was to arise, OpaL's design is highly amenable to directed evolution. Because OpaL's aggregation centrally depends on its hydrophobic characteristics, mutations should be less likely to decrease OpaL's activity, widening the pool of potentially improved mutants as compared to most protein therapeutics. After iterated mutagenesis, opaL may regain activity against resistant pathogens. Mutations in opaL's promoter may enable outgrowth, but donors with fresh copies of the original opaL could be introduced to restore full expression. Given that hydrophobic aggregation can occur in any aqueous cellular environment, OpaL may exhibit activity in diverse types of bacteria. This technology provides new opportunities for addressing antibiotic-resistant infections.

ASSOCIATED CONTENT

S Supporting Information

The Supporting Information is available free of charge on the ACS Publications website at DOI: 10.1021/acs.biochem.8b00888.

Supplementary background on conjugative plasmids, detailed materials and methods, amino acid sequence of OpaLacidic, plasmid maps, protein extracted from OpaL, OpaLacidic, and Δ OpaL run on 8% Tris-glycine polyacrylamide gels, comparison of plates for the mating-toxicity experiment, strains, plasmids, and experiments in which each strain was utilized, and percent aggregation propensities (PDF)

AUTHOR INFORMATION

Corresponding Author

*E-mail: chatterjee@colorado.edu. Phone: (303) 735-6586. Fax: (303) 492-8425.

ORCID

Anushree Chatterjee: 0000-0002-8389-9917

Author Contributions

A.C. supervised the project. L.C., P.O., C.M.C., and A.C. designed the research. L.C. and J.C. performed the experiments and the statistical data analysis. L.C., A.C., P.O., and C.M.C. wrote the manuscript.

Funding

This work has been supported by the National Science Foundation award no. MCB1714564 to A.C. P.O. and C.M.C. were supported by National Science Foundation Fellowships.

Notes

The authors declare no competing financial interest.

ACKNOWLEDGMENTS

The imaging work was performed at the BioFrontiers Institute Advanced Light Microscopy Core with the help of Joe Dragavon. Laser scanning confocal microscopy was performed on a Nikon A1R microscope supported by NIST-CU Cooperative Agreement award no. 70NANB15H226. The funders had no role in the study design, data collection and analysis, decision to publish, or preparation of the manuscript.

REFERENCES

- (1) Kumarasamy, K. K., Toleman, M. A., Walsh, T. R., Bagaria, J., Butt, F., Balakrishnan, R., Chaudhary, U., Doumith, M., Giske, C. G., Irfan, S., et al. (2010) *Lancet Infect. Dis.* 10 (9), 597–602.
- (2) Stefani, M., and Dobson, C. M. (2003) J. Mol. Med. (Heidelberg, Ger.) 81 (11), 678-699.
- (3) Bednarska, N. G., van Eldere, J., Gallardo, R., Ganesan, A., Ramakers, M., Vogel, I., Baatsen, P., Staes, A., Goethals, M., Hammarström, P., et al. (2016) *Mol. Microbiol.* 99 (5), 849–865.
- (4) Khodaparast, L., Khodaparast, L., Gallardo, R., Louros, N. N., Michiels, E., Ramakrishnan, R., Ramakers, M., Claes, F., Young, L., and Shahrooei, M. (2018) *Nat. Commun.* 9 (1), 866.
- (5) Fernandez-Escamilla, A.-M., Rousseau, F., Schymkowitz, J., and Serrano, L. (2004) *Nat. Biotechnol.* 22 (10), 1302–1306.
- (6) Schwartz, R., Istrail, S., and King, J. (2008) Protein Sci. 10 (5), 1023–1031.
- (7) Turoverov, K. K., Kuznetsova, I. M., and Uversky, V. N. (2010) *Prog. Biophys. Mol. Biol.* 102 (2), 73–84.
- (8) Bertoncini, C. W., Jung, Y.-S., Fernandez, C. O., Hoyer, W., Griesinger, C., Jovin, T. M., and Zweckstetter, M. (2005) *Proc. Natl. Acad. Sci. U. S. A.* 102 (5), 1430–1435.
- (9) Ramshini, H., Parrini, C., Relini, A., Zampagni, M., Mannini, B., Pesce, A., Saboury, A. A., Nemat-Gorgani, M., and Chiti, F. (2011) *PLoS One* 6 (1), No. e16075.
- (10) Wickner, S., Maurizi, M. R., and Gottesman, S. (1999) Science 286 (5446), 1888–1893.
- (11) Tobias, J. W., Shrader, T. E., Rocap, G., and Varshavsky, A. (1991) Science 254 (5036), 1374–1377.
- (12) Ross, C. A., and Poirier, M. A. (2004) Nat. Med. 10, S10.
- (13) Bednarska, N. G., Schymkowitz, J., Rousseau, F., and Van Eldere, J. (2013) Microbiology 159 (Pt 9), 1795–1806.
- (14) Demeule, B., Gurny, R., and Arvinte, T. (2007) Int. J. Pharm. 329 (1-2), 37-45.
- (15) Adamczyk, M., and Jagura-Burdzy, G. (2003) Acta Biochim. Polym. 50 (2), 425–453.
- (16) Ingram, L. C., Richmond, M. H., and Sykes, R. B. (1973) Antimicrob. Agents Chemother. 3 (2), 279–288.

Biochemistry

(17) Pansegrau, W., Lanka, E., Barth, P. T., Figurski, D. H., Guiney, D. G., Haas, D., Helinski, D. R., Schwab, H., Stanisich, V. A., and Thomas, C. M. (1994) *J. Mol. Biol.* 239 (5), 623–663.

- (18) Bordoy, A. E., Varanasi, U. S., Courtney, C. M., and Chatterjee, A. (2016) ACS Synth. Biol. 5 (12), 1331–1341.
- (19) Romero, P. A., and Arnold, F. H. (2009) Nat. Rev. Mol. Cell Biol. 10 (12), 866-876.
- (20) de la Cruz, F., Frost, L. S., Meyer, R. J., and Zechner, E. L. (2010) FEMS Microbiol. Rev. 34 (1), 18-40.